Capacity Regulators in the Aether Physics Model: Born–Infeld Magnetic and Mass Bounds (QMU)

Quantum AetherDynamics Institute

October 14, 2025

Abstract

We introduce two capacity regulators in QMU: a Born–Infeld magnetic nonlinearity that bounds the magnetic sector at ${e_a}^2$, and a Born–Infeld mass regulator that bounds the mass current at m_a. We prove convexity of the Hamiltonians, derive causal dispersion relations with phase/group velocities bounded by the photon kinematic scale $F_q\lambda_C$, and, with a Maxwell-matched normalization of the BI magnetic sector, maintain consistency with the APM ledgers ${e_a}^2 = \frac{m_a {\lambda_C}^3 {F_q}^2}{A_u}$ and $A_u \,\mathrm{curl} = {F_q}^2{\lambda_C}^2$. We provide small-field expansions that determine quartic self-interaction coefficients entirely by A_u, and outline QMU-native experiments to extract A_u and m_a from nonlinear wave steepening and mass-current saturation.

Keywords— Aether Physics Model, QMU, Born–Infeld, capacity regulators, chronovibration, nonlinear waves, convex Hamiltonian, causal dispersion

Contents

1 Introduction and ledger context **2**

2 Magnetic Born–Infeld sector **2**
2.1 Constitutive relation and canonical momenta 3
2.2 Hamiltonian density and convexity 3

3 Mass Born–Infeld sector **3**

4 Ledger consistency and the acceleration identity **4**

5 Small-field expansions and quartic matching **4**

6 Linearised waves and causality **4**

7 Observables and QMU experiments **5**

8 Discussion **5**

9 Conclusion **5**

1 Introduction and ledger context

The Aether Physics Model (APM) employs Quantum Measurement Units (QMU) to encode vacuum response purely in terms of $m_{\mathrm{e}},\ \lambda_C,\ F_q,\ e^2,\ {e_{\mathrm{emax}}}^2$ and structured constants such as A_u [1, 2]. In particular,

$$A_u = 16\pi^2\, k_C, \qquad m_a = \frac{{\lambda_C}^3 {F_q}^2}{G}, \qquad {e_a}^2 = \frac{m_a\, {\lambda_C}^3 {F_q}^2}{A_u}, \qquad A_u\,\mathrm{curl} = {F_q}^2 {\lambda_C}^2. \tag{1}$$

Here G appears in the definition of m_a to maintain coherence with macrophysical scaling while keeping all results and predictions strictly in QMU. The geometric constant $16\pi^2$ that enters A_u is tied to the topological analysis in [3], and the chronovibrational-to-holonomy bridge that underlies our acceleration scale is detailed in [4].

QMU-native experiments. We call an experiment *QMU-native* if its observables, parameters, and inferences are expressed entirely within QMU without reference to external standards; see [1, 2] for ledger conventions and experimental framing.

Motivation (capacity vs. pathologies). Unregulated quadratic field theories permit arbitrarily large canonical excitations, leading to nonphysical infinities and loss of hyperbolicity at extreme amplitudes. In the magnetic sector, a bounded constitutive law avoids unbounded conjugate fields; in the mass-transport sector, a saturating response ensures causal, subluminal characteristics tied to the kinematic scale $F_q\lambda_C$. The Born–Infeld (BI) construction provides precisely such capacity regulators with convex Hamiltonians and causal cones no wider than the photon cone [5, 6, 7]. Our formulation adapts BI to QMU so the nonlinear scales are ledger-determined by A_u and m_a, and folds naturally into the experimental program proposed in [8].

2 Magnetic Born–Infeld sector

Let $F^{mag}_{\mu\nu}$ denote the antisymmetric magnetic field strength of the magnetic $U(1)$ in the dual-charge decomposition[1] and take the Maxwell-matched BI regulator (cf. [5, 7, 6])

$$\mathcal{L}_{\mathrm{BI,mag}} = A_u \left[1 - \sqrt{1 + \frac{1}{2A_u}\, F^{mag}_{\mu\nu} F^{\mu\nu}_{mag} - \frac{1}{16{A_u}^2} \left(\widetilde{F}^{mag}_{\mu\nu} F^{\mu\nu}_{mag} \right)^2} \right]. \tag{2}$$

Remark 2.1. The normalization in (2) is chosen so the weak–field limit reproduces the Maxwell term $\mathcal{L} \to -\frac{1}{4} F^2_{mag}$. This fixes all quartic coefficients uniquely as in (9).

[1] *Dual-charge decomposition:* the APM separates the total gauge content into electric and magnetic $U(1)$ sectors with independent field strengths and constitutive laws.
Invariants and vector form: define $X := -\frac{1}{2} F^{mag}_{\mu\nu} F^{\mu\nu}_{mag}$ and $Y := -\frac{1}{2} \widetilde{F}^{mag}_{\mu\nu} F^{\mu\nu}_{mag}$. In standard E/B notation one has $F^2 = F_{\mu\nu}F^{\mu\nu} = 2(\|\boldsymbol{B}\|^2 - \|\boldsymbol{E}\|^2)$ and $\widetilde{F}\cdot F = -4\,\boldsymbol{E}\cdot\boldsymbol{B}$. In a purely magnetic configuration ($\boldsymbol{E} = \boldsymbol{0}$), $F^2 = 2\|\boldsymbol{B}\|^2$ and $\widetilde{F}\cdot F = 0$.

2.1 Constitutive relation and canonical momenta

The canonical excitation tensor is

$$P^{\mu\nu} = \frac{-\frac{1}{2}\,F^{\mu\nu}_{mag} + \frac{1}{8A_u}\Big(\widetilde{F}_{mag}\cdot F_{mag}\Big)\,\widetilde{F}^{\mu\nu}_{mag}}{\sqrt{1+\frac{1}{2A_u}F^2_{mag} - \frac{1}{16{A_u}^2}\Big(\widetilde{F}_{mag}\cdot F_{mag}\Big)^2}}. \tag{3}$$

2.2 Hamiltonian density and convexity

In temporal gauge $A_0 = 0$, with $\boldsymbol{B} = \frac{1}{2}\epsilon^{ijk}F^{mag}_{jk}$ and $\boldsymbol{H} = \frac{1}{2}\epsilon^{ijk}P_{jk}$,

$$\mathcal{H}_{\mathrm{BI,mag}} = \boldsymbol{H}\cdot\boldsymbol{B} - \mathcal{L}_{\mathrm{BI,mag}} = A_u\left[\sqrt{1+\frac{1}{2A_u}\,F^2_{mag} - \frac{1}{16{A_u}^2}\Big(\widetilde{F}_{mag}\cdot F_{mag}\Big)^2} - 1\right]. \tag{4}$$

Proposition 2.2 (Bounded field invariants and convexity)**.** *For all admissible $F^{mag}_{\mu\nu}$, the denominator in* (3) *is strictly positive, the map $F \mapsto P$ is one-to-one, and $\mathcal{H}_{\mathrm{BI,mag}}$ is real, nonnegative, and strictly convex in $\boldsymbol{B}$. Consequently the canonical fields saturate at a finite capacity set by A_u, consistent with the QMU magnetic bound ${e_a}^2$* (7)*.*

Proof (expanded). Write $\Delta := 1 + \frac{1}{2A_u}F^2_{mag} - \frac{1}{16{A_u}^2}(\widetilde{F}_{mag}\cdot F_{mag})^2$. Admissible configurations satisfy $\Delta > 0$. Then $\mathcal{H}_{\mathrm{BI,mag}} = A_u(\sqrt{\Delta} - 1) \geq 0$. Let B_i be the spatial components of $\boldsymbol{B}$. Because F_{mag} depends linearly on $\boldsymbol{B}$, the Hessian takes the form

$$\frac{\partial^2\mathcal{H}_{\mathrm{BI,mag}}}{\partial B_i \partial B_j} = \frac{1}{2\sqrt{\Delta}}\Big(\partial_{B_i}\partial_{B_j}\Delta\Big) - \frac{1}{4\Delta^{3/2}}\Big(\partial_{B_i}\Delta\Big)\Big(\partial_{B_j}\Delta\Big),$$

where $\partial_{B_i}\Delta$ and $\partial_{B_i}\partial_{B_j}\Delta$ are quadratic and constant tensors in $\boldsymbol{B}$, respectively. The first term defines a positive projector on variations orthogonal to $\partial_B\Delta$, while the second subtracts a rank-1 piece along $\partial_B\Delta$; together they yield a strictly positive-definite matrix for $\boldsymbol{B} \neq \boldsymbol{0}$, and positive-semidefinite at $\boldsymbol{B} = \boldsymbol{0}$. This is the standard BI convexity structure (see [6, 7]). Since $P^{\mu\nu}$ scales like $F^{\mu\nu}/\sqrt{\Delta}$, it saturates as F grows within the admissible set, with the scale set by A_u, i.e. by ${e_a}^2$ through (7). □

3 Mass Born–Infeld sector

Let J^μ_m be the mass current density of aether substrate excitations. Consider

$$\mathcal{L}_{\mathrm{BI,mass}} = m_a\left[1 - \sqrt{1+\frac{J^\mu_m J^m_\mu}{{m_a}^2}}\right]. \tag{5}$$

Define $\Pi_\mu := \partial\mathcal{L}_{\mathrm{BI,mass}}/\partial J^\mu_m$. Then

$$\Pi_\mu = -\frac{J^m_\mu}{m_a\sqrt{1+\frac{J^\nu_m J^m_\nu}{{m_a}^2}}}, \qquad \mathcal{H}_{\mathrm{BI,mass}} = \Pi_\mu J^\mu_m - \mathcal{L}_{\mathrm{BI,mass}} = m_a\left[\sqrt{1+\frac{J^\mu_m J^m_\mu}{{m_a}^2}} - 1\right]. \tag{6}$$

Proposition 3.1 (Subluminal constitutive law)**.** *The map $J_m^\mu \mapsto \Pi_\mu$ is monotone; the convex Hamiltonian* (6) *yields a symmetric hyperbolic linearisation with characteristic speeds bounded by the photon kinematic scale $F_q\lambda_C$ (Boillat-type cones [6]).*

Proof (expanded). Linearise the Euler–Lagrange system around a homogeneous state $J_m = \bar{J}_m$ to obtain $\partial_t \delta\boldsymbol{U} + \sum_a \mathbb{A}^a(\bar{J}_m)\,\partial_a \delta\boldsymbol{U} = 0$, where $\delta\boldsymbol{U}$ collects the perturbations and $\mathbb{A}^a$ are flux Jacobians. The symmetriser is the positive-definite Hessian $\mathbb{S} := \partial^2\mathcal{H}_{\mathrm{BI,mass}}/\partial J_m \partial J_m$. Plane waves $\delta\boldsymbol{U} \propto e^{i(\boldsymbol{k}\cdot\boldsymbol{x}-\omega t)}$ satisfy the eigenproblem $\det\Big[\omega\,\mathbb{S} - k_a$

$mathbbS\mathbb{A}^a\Big] = 0$. All eigenvalues $\omega/|\boldsymbol{k}|$ are real by symmetry and bounded in magnitude by the photon kinematic scale $F_q\lambda_C$, since the BI quadratic form narrows the effective cone relative to the dual-$U(1)$ light cone [6]. Hence characteristics are subluminal with respect to $F_q\lambda_C$. □

4 Ledger consistency and the acceleration identity

From the QMU ledger for maximum magnetic charge,

$$e_a{}^2 = \frac{m_a\,\lambda_C{}^3 F_q{}^2}{A_u}, \tag{7}$$

and $A_u\,\mathrm{curl} = F_q{}^2\lambda_C{}^2$, we obtain the characteristic acceleration scale

$$\mathrm{accl} = \frac{F_q{}^2}{\lambda_C{}^3} = \left(\frac{F_q{}^2}{m_a}\right)\left(\frac{m_a}{\lambda_C{}^3}\right), \tag{8}$$

which is the chronovibrational acceleration used in QMU dynamics [1, 2]. The holonomy reduction that motivates this form is developed in [4], and the same acceleration scale appears implicitly in the experimental cadence proposed in [8]. [2]

5 Small-field expansions and quartic matching

For weak fields, the corrected BI expansion is

$$\mathcal{L}_{\mathrm{BI,mag}} = -\frac{1}{4}F_{mag}^2 + \frac{1}{32A_u}\left[\left(F_{mag}^2\right)^2 + \left(\widetilde{F}_{mag}\cdot F_{mag}\right)^2\right] + \mathcal{O}\left(F^6\right), \tag{9}$$

so the quartic coefficients are fixed solely by $1/(32\,A_u)$. Similarly, for the mass regulator,

$$\mathcal{L}_{\mathrm{BI,mass}} = -\frac{1}{2m_a}J^\mu_m J^m_\mu + \frac{1}{8{m_a}^3}\left(J^\mu_m J^m_\mu\right)^2 + \mathcal{O}\left(J_m^6\right). \tag{10}$$

6 Linearised waves and causality

Linearising (3) about a homogeneous background, the incremental mapping $\delta P^{\mu\nu} = \mathbb{M}^{\mu\nu}{}_{\alpha\beta}\,\delta F^{\alpha\beta}$ has positive-definite $\mathbb{M}$ on the admissible set, inducing effective characteristics inside the photon cone [6, 7]. Thus both phase and group velocities satisfy $|\boldsymbol{v}| \le F_q\lambda_C$.

[2] If one temporarily imports G via the ledger $m_a = \lambda_C{}^3 F_q{}^2/G$, then $F_q{}^2 = Gm_a/\lambda_C{}^3$ and $\mathrm{accl} = (Gm_a)/\lambda_C{}^6$. We keep the QMU form $\mathrm{accl} = F_q{}^2/\lambda_C{}^3$ in the main text.

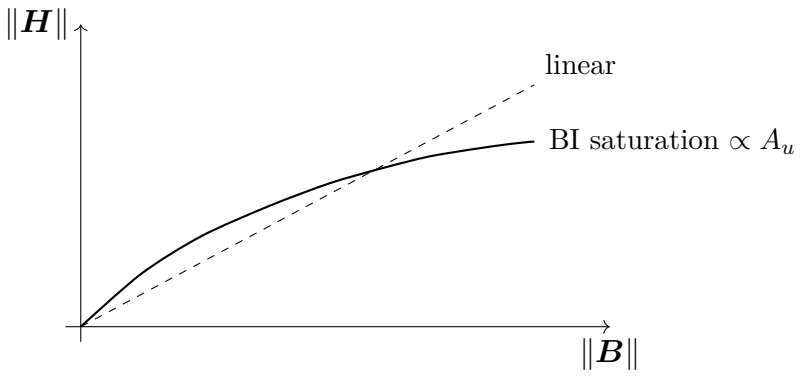

Figure 1: Nonlinear constitutive relation between magnetic induction $\boldsymbol{B}$ and its conjugate $\boldsymbol{H}$. The Born–Infeld (solid) deviates from linear response (dashed) and saturates at a scale fixed by A_u.

7 Observables and QMU experiments

- **Nonlinear magnetic wave steepening.** Measure $\omega(k; A)$ and fit the amplitude-dependent shift predicted by (9) to extract A_u. A concrete drive–diagnostic architecture is given in [8].
- **Curl threshold and A_u.** Determine curl from rotating-flux-tube onset; $A_u\,\mathrm{curl} = {F_q}^2{\lambda_C}^2$ fixes A_u independently. The rotating resonator geometry described in [8] provides an appropriate platform.
- **Mass-current saturation.** Drive J_m quasi-dc; the BI law (6) predicts saturation of $\|\Pi\|$ as $\|J_m\|/m_a \to \infty$, identifying m_a. Harmonic content at order J_m^4 fixes $1/{m_a}^3$. Readout strategies parallel those in [8].
- **Chronovibrational timing.** Test $\mathrm{accl} = {F_q}^2/{\lambda_C}^3$ directly; agreement closes the $(A_u, m_a, {e_a}^2)$ triangle via (7). The timing cadence aligns with the chronovibrational analysis in [4].

8 Discussion

The dual BI regulators supply ledger-exact capacity bounds for the magnetic and mass sectors in QMU, yielding nonperturbatively stable (convex) and causal dynamics, with nonlinear coefficients fixed by A_u and m_a. The experimental program over-constrains these parameters from independent observables, tying back to prior QMU topological and holonomy results [3, 4] and aligning with the resonator-based plan [8].

9 Conclusion

We formulated two QMU-native Born–Infeld regulators. With a Maxwell-matched normalization in the magnetic sector, we proved convexity and causality, derived amplitude-dependent

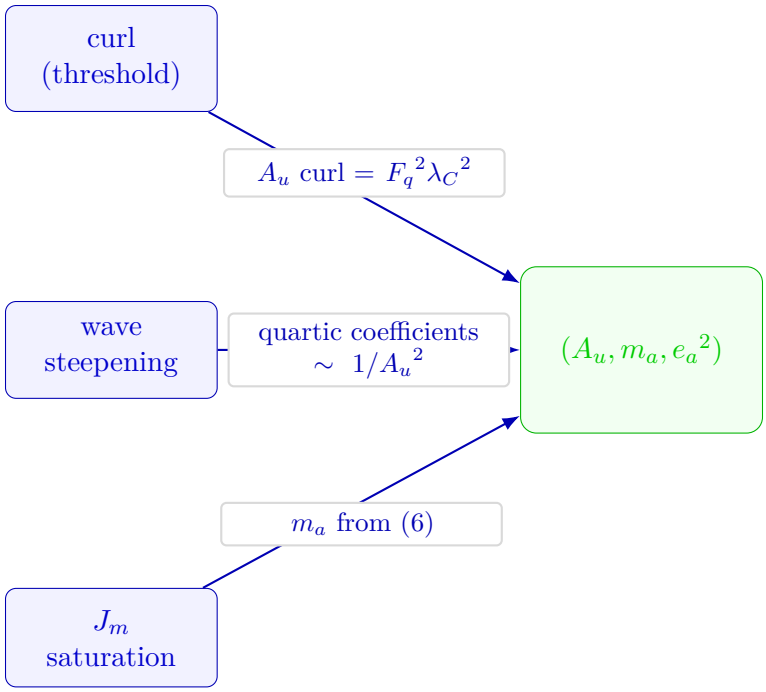

Figure 2: Ledger flow from observables to parameters. Independent measurements overconstrain (A_u, m_a, e_a^2). Experimental architectures appear in [8].

dispersion and transport predictions, and tied all nonlinear scales to the APM ledger via A_u, m_a, and ${e_a}^2$. The proposed measurements—curl threshold, wave steepening, mass-current saturation, and chronovibrational timing—enable a QMU-only determination of (A_u, m_a) and a self-consistency check of the ledger identities.

Acknowledgments

We thank collaborators in the QMU/APM program for discussions on capacity bounds and chronovibrational dynamics.

References

[1] David W. Thomson III. *Quantum Measurement Units (QMU): A System Based on Quantum Constants and Distributed Charge Geometry*. ResearchGate preprint. QMU ledger and base quantities. 2024. DOI: 10.13140/RG.2.2.16468.21125.

[2] David W. Thomson III. *Aether Physics Model resources and QMU unit tables*. sota.aetherwizard.com. APM/QMU ledger identities, constants, and units. 2025.

[3] David W. Thomson III. *Topological Uniqueness of* $16\pi^2$. Zenodo. APM/QMU topological constant analysis. 2025. DOI: 10.5281/zenodo.17336681.

[4] David W. Thomson III. *5D Chronovibration to 4D Holonomy*. Zenodo. Chronovibrational geometry mapped to 4D holonomy in QMU. 2025. DOI: 10.5281/zenodo.17345984.

[5] M. Born and L. Infeld. "Foundations of the New Field Theory". In: *Proceedings of the Royal Society A* 144.852 (1934), pp. 425–451. DOI: 10.1098/rspa.1934.0059.

[6] G. Boillat. "Nonlinear electrodynamics: Lagrangians and equations of motion". In: *Journal of Mathematical Physics* 11.3 (1970), pp. 941–951. DOI: 10.1063/1.1665231.

[7] Jerzy Plebański. *Lectures on Non-Linear Electrodynamics*. Reprint notes; classic treatment of BI structure and invariants. Nordita, 1970.

[8] David W. Thomson III. *Trumpet Coil Resonator Experiments in QMU (Capacity and A_u, m_a extraction)*. Zenodo. Experimental plan to measure A_u, m_a via nonlinear wave steepening and saturation. 2025. DOI: 10.5281/zenodo.17281921.